

Tunable Luminescent Lanthanide Coordination Polymers Based on Reversible Solid-State Ion-Exchange Monitored by Ion-Dependent Photoinduced Emission Spectra

Peng Wang, Jian-Ping Ma, Yu-Bin Dong,* and Ru-Qi Huang

College of Chemistry, Chemical Engineering and Materials Science, Engineering Research Center of Pesticide and Medicine Intermediate Clean Production, Ministry of Education, Shandong Normal University, Jinan 250014, P. R. China

Received April 7, 2007; E-mail: yubindong@sdu.edu.cn

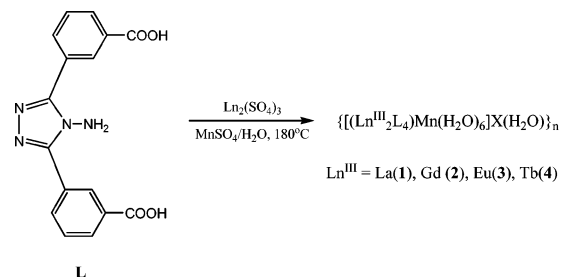
The study of coordination-driven self-assembled polymeric metal–organic frameworks (MOFs) is a very active interdisciplinary research area.¹ Such supramolecular assemblies have intriguing structures as well as potential applications as smart optoelectronic, magnetic, catalytic, and porous materials. To our knowledge, only a handful of lanthanide-based porous MOFs which are able to uptake and release guest species in a reversible manner have been reported.² In addition, IR, NMR, XRD, and single-crystal analysis are the main monitoring techniques to characterize reversible solid-state guest-exchange processes.³ Up to now, however, the luminescence properties have rarely been used to monitor guest-exchange processes.^{4b} The guest-dependent photoinduced emission spectra not only offer a facile monitoring technique to characterize solid-state guest-exchange processes but also provide a practical approach to access of tunable fluorescent materials.

Motivated by our interest in selective and reversible guest-exchange chemistry based on porous MOFs, we have initiated a synthetic program for the preparation of open MOFs, in which the bent five-membered heteroatom-ring-bridged ligands are chosen as the building blocks.⁴ We present here the first family of lanthanide-based MOFs consisting of the nanosized Ln₂L₄ cage-like units which encapsulate the [Mn(H₂O)₆]²⁺ cations. These porous coordination polymers can remain intact upon reversible ion-exchange with different Ln(III) cations, which was characterized by the ion-dependent photoinduced emission spectra and XRD patterns.

As shown in Scheme 1, reactions of the bent 1,2,4-trizole bridging ligand L with Ln₂(SO₄)₃·8H₂O in the presence of MnSO₄·H₂O under hydrothermal conditions (H₂O, 180 °C), afforded the compounds {[Ln^{III}₂L₄]Mn(H₂O)₆·x(H₂O)}_n (Ln(III) = La (1), Gd (2), Eu (3), and Tb (4)) as colorless crystals in good yield (Supporting Information). Single-crystal analysis (Supporting Information) revealed that 1–4 feature a similar 1D chain motif. For example, the structure of 2 contains two crystallographically independent Gd(III) atoms, which are both found in eight-coordinated dodecahedral coordination spheres that are composed of eight carboxylate oxygen donors from six L ligands (Figure 1). The four of eight carboxylate groups from four L ligands behave as the μ₂-bridge to bind two Gd(1) ions together, resulting in a Gd₂O₁₆ cluster with a close Gd(1)···Gd(1) contact of ~4.0 Å. Such coordination mode plays a central role in the formation of 2 with a neutral 1D polymeric framework (Figure 1). The Gd–O bond distances range from 2.337(4) to 2.677(4) Å.

The most important structural feature of 1–4 is that these neutral 1D polymeric chains consist of the Ln₂L₄ tetragonal prisms^{4b} enclosing the [Mn(H₂O)₆]²⁺ cations (Figure 1). As shown in Figure 1, four bent L ligands bridge two Ln(2) ions to form the tetragonal prismatic cage. The dodecahedral coordination mode of Gd(III) center prevents a symmetric alignment of the L spacers,

Scheme 1. The Synthesis of Ln(III)-Coordination Polymers 1–4



leading to the tetragonal prism being twisted. This structural arrangement leaves openings of 6.8–7.1 Å in the side of the cage. One distorted octahedral [Mn(H₂O)₆]²⁺ cation is trapped inside and is hydrogen-bonded to the framework carboxylate moieties (Figure 1). Within the cage, the Gd···Gd distance is ~11 Å and the distance between the two opposite trizole rings is ~10 Å.

In the solid state, the Gd₂L₄ cage-containing chains extend along the crystallographic *c*-axis. As indicated in Figure 2, the tetragonal cage-like units permit the chains to arrange tidily in the crystallographic *ab* plane, generating the squarelike channels along the chain direction. Uncoordinated water molecules are located inside. When viewed down the crystallographic [110] direction, rectangular channels (crystallographic dimensions, 7.8 × 7.0 Å) are evident in 2 (Figure 2). So far, a number of 1D metal-organic polymers have been reported, 1D coordination polymers composed of the nanosized Ln₂L₄ tetragonal prisms, however, are unprecedented.

Coordination-driven lanthanide complexes have attracted considerable attention as promising sensory materials because of their intense luminescence.⁵ The luminescence spectra of 1–4 were

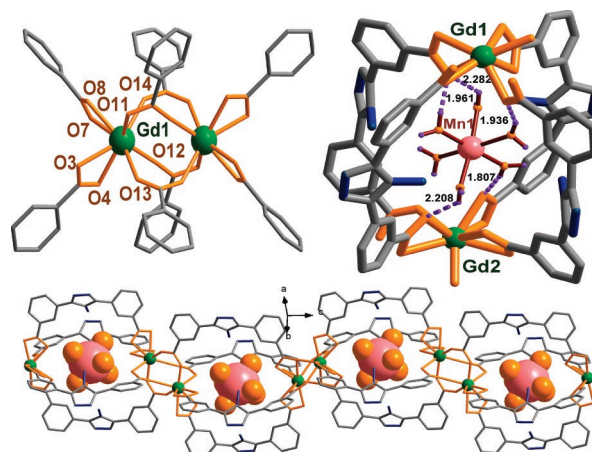


Figure 1. (Top-left) The coordination sphere of Gd(III); (top-right) the cage unit encapsulating [Mn(H₂O)₆]²⁺ guest; (bottom) the 1D chain in 2.

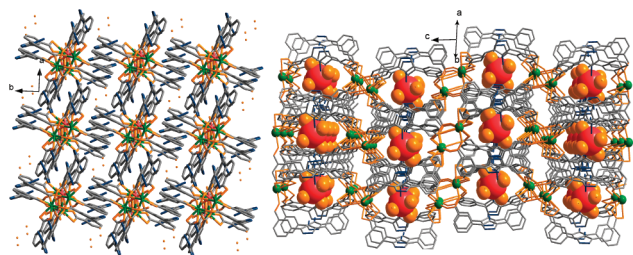


Figure 2. The solid state arrangement in **2**, viewed parallel (left) and perpendicular (right) to the chains.

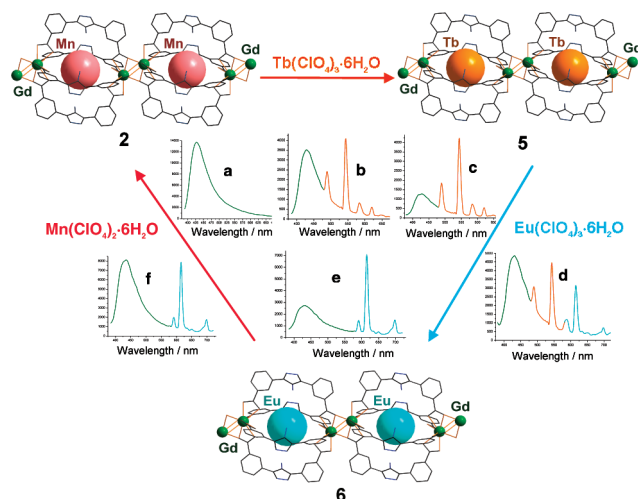


Figure 3. Guest-exchanging process of cation species based on **2**: (a–c) the solid-state emission spectra ($\lambda_{\text{ex}} = 368$ nm) of **2** stirred in a $\text{Tb}(\text{ClO}_4)_3$ aqueous solution at 0, 2, and 7 days, respectively; (c–e) the solid-state emission spectra ($\lambda_{\text{ex}} = 368$ nm) of **5** stirred in a $\text{Eu}(\text{ClO}_4)_3$ aqueous solution at 0, 2, and 7 days, respectively; (e–a) show the solid-state emission spectra ($\lambda_{\text{ex}} = 368$ nm) of **6** stirred in a $\text{Mn}(\text{ClO}_4)_2$ aqueous solution at 0, 2, and 7 days, respectively. The emission bands of **2**, **5**, and **6** are shown in green, orange, and cyan, respectively.

measured in the solid state. The fluorescence of **1** ($\lambda_{\text{ex}} = 397$ nm) and **2** ($\lambda_{\text{ex}} = 368$ nm) exhibit one emission maximum at 459 and 428 nm, respectively. Compared to the ligand emission (510 nm), the blue-shift luminescence of **1** and **2** is believed to be based upon ligand-to-metal-charge-transfer (LMCT).⁶ Different from **1** and **2**, compounds **3** and **4** provide typical emission band features. For **3**, the emission bands arise from the $^5\text{D}_0 \rightarrow ^7\text{F}_J$ ($J = 1, 2, 3, 4$) transitions of $\text{Eu}(\text{III})$. The corresponding emission bands are 578, 589, 611, 698 nm, respectively. Among these transitions, $^5\text{D}_0 \rightarrow ^7\text{F}_2$ is the strongest. For **5**, four lines of $\text{Tb}(\text{III})$ emission can be detected in the visible spectrum, corresponding to transitions from the $^5\text{D}_4$ state: $^5\text{D}_4 \rightarrow ^7\text{F}_6$ (489 nm), $^5\text{D}_4 \rightarrow ^7\text{F}_5$ (542 nm), $^5\text{D}_4 \rightarrow ^7\text{F}_4$ (585 nm), and $^5\text{D}_4 \rightarrow ^7\text{F}_3$ (620 nm). The most prominent line was observed at 542 nm (Supporting Information).

The porous frameworks of **1–4** are able to undergo a reversible and controllable cation-exchange. The encapsulated $[\text{Mn}(\text{H}_2\text{O})_6]^{2+}$ species are readily replaced reversibly by the $[\text{Ln}(\text{H}_2\text{O})_8]^{3+}$ cations with preservation of the original crystal structure, which leads to luminescence tunability. For example, the crystals of **2** were stirred in an aqueous solution of $\text{Tb}(\text{ClO}_4)_3 \cdot 6\text{H}_2\text{O}$ (large excess) at room temperature for 7 days, generating a new host–guest complex $\{[(\text{Gd}_2\text{L}_4)\text{Tb}(\text{H}_2\text{O})_8\text{ClO}_4] \cdot 0.5(\text{H}_2\text{O})\}_n$ (**5**). As shown in Figure 3, both emission bands of **2** and **5** are found in the emission spectrum after 2 days, which indicates that the encapsulated $[\text{Mn}(\text{HO}_2)_6]^{2+}$

in **2** were partially replaced by the $[\text{Tb}(\text{H}_2\text{O})_8]^{3+}$ cations. As time goes on, the typical emission intensities of **5** increased, while the intensity of the fluorescence of **2** decreased. After 7 days, no more changes for the fluorescent intensities have been observed, indicating that the exchange reaction of Mn^{II} by Tb^{III} was finished. The XRD pattern of **5** indicates that the solid structure of **2** is maintained upon ion-exchange (Supporting Information). Besides the $\text{Ln}(\text{ClO}_4)_3$, the LnCl_3 or $\text{Ln}(\text{NO}_3)_3$ can also be used to perform the ion-exchange reactions, but takes a longer time (Supporting Information). Furthermore, the $\text{Tb}(\text{III})$ cation in **5** can be replaced by its analogue. For example, the crystals of **5** were stirred in an aqueous solution of $\text{Eu}(\text{ClO}_4)_3 \cdot 6\text{H}_2\text{O}$ (large excess) at room temperature for 7 days to generate the new complex $\{[(\text{Gd}_2\text{L}_4)\text{Eu}(\text{H}_2\text{O})_8\text{ClO}_4] \cdot 0.5(\text{H}_2\text{O})\}_n$ (**6**), in which the $[\text{Eu}(\text{H}_2\text{O})_8]^{3+}$ species are located. The emission spectra (Figure 3) and XRD pattern (Supporting Information) demonstrate this ion-exchange process well. More interesting is that **2** can be regenerated when **6** was treated by a large excess of $\text{Mn}(\text{ClO}_4)_2 \cdot 6\text{H}_2\text{O}$ in water for 7 days, which is well confirmed by the XRD pattern and emission spectrum (Supporting Information). Compounds **1–4** are completely insoluble in water owing to their polymeric natures (Supporting Information), so the possibility of a dissolution–recrystallization mechanism for explaining this reversible guest-exchange is impossible.

In conclusion, a series of 1D lanthanide-based coordination polymers consisting of Ln_2L_4 cage units with tunable luminescent properties based on reversible ion-dependent exchange was reported. Most importantly, it provides a promising and convenient approach to access the multifunctional luminescent materials that can provide tunable emissions by controlling the type of guest species. We believe that such a property should lead to new, tunable fluorescent materials and sensors.

Acknowledgment. We are grateful for financial support from the National Natural Science Foundation of China (Grant No. 20671060), National Basic Research Program of China (973 Program, 2007CB936000), and Shandong Natural Science Foundation (Grant Nos. Z2004B01, J06D05 and 2006BS04040).

Supporting Information Available: Crystallographic data and CIF files of **1–4**, synthesis, emission spectra, TGA traces of **1–4**, and XRD patterns of **5**, **6**, and **2'**. This material is available free of charge via the Internet at <http://pubs.acs.org>.

References

- (1) (a) Moulton, B.; Zaworotko, M. J. *Chem. Rev.* **2001**, *101*, 1629. (b) Yaghi, O. M.; O'Keeffe, M.; Ockwig, N. W.; Chae, H. K.; Eddaoudi, M.; Kim, J. *Nature* **2003**, *423*, 706. (c) Kitagawa, S.; Kitaura, R.; Noro, S.-I. *Angew. Chem., Int. Ed.* **2004**, *43*, 2334.
- (2) (a) Wong, K.-L.; Law, G.-L.; Yang, Y.-Y.; Wong, W.-T. *Adv. Mater.* **2006**, *18*, 1051. (b) Devic, T.; Serre, C.; Audebrand, N.; Marrot, J.; Férey, G. *J. Am. Chem. Soc.* **2005**, *127*, 12788. (c) Chen, C.-L.; Goforth, A.; Smith, M. D.; Su, C.-Y.; zur Loye, H.-C. *Angew. Chem., Int. Ed.* **2005**, *44*, 6643.
- (3) (a) Ohmori, O.; Kawano, M.; Fujita, M. *J. Am. Chem. Soc.* **2004**, *126*, 16292. (b) Min, K. S.; Suh, P. M. *J. Am. Chem. Soc.* **2000**, *122*, 6834. (c) Hamilton, B. H.; Kelly, K. A.; Wagler, T. A.; Espe, M. P.; Ziegler, C. J. *Inorg. Chem.* **2004**, *43*, 50.
- (4) (a) Dong, Y.-B.; Zhang, Q.; Liu, L.-L.; Ma, J.-P.; Tang, B.; Huang, R.-Q. *J. Am. Chem. Soc.* **2007**, *129*, 1514. (b) Dong, Y.-B.; Wang, P.; Ma, J.-P.; Zhao, X.-X.; Wang, H.-Y.; Tang, B.; Huang, R.-Q. *J. Am. Chem. Soc.* **2007**, *129*, 4872.
- (5) (a) Bünzli, J.-C. *Acc. Chem. Res.* **2006**, *39*, 53. (b) Petoud, S.; Cohen, S. M.; Bünzli, J.-C. G.; Raymond, K. N. *J. Am. Chem. Soc.* **2003**, *125*, 13324. (c) Weibel, N.; Charbonnière, L. J.; Guardigli, M.; Roda, A.; Ziessel, R. *J. Am. Chem. Soc.* **2004**, *126*, 4888.
- (6) Chatterton, N.; Bretonnière, Y.; Pécaut, J.; Mazzanti, M. *Angew. Chem., Int. Ed.* **2005**, *44*, 7595.

JA072442H